Terahertz difference frequency response of pdd in two-laser experiments

TERAHERTZ DIFFERENCE FREQUENCY RESPONSE OF PDD IN TWO-LASER EXPERIMENTS

P. L. HAGELSTEIN[1], D. LETTS[2] and D. CRAVENS[3]
[1] *Research Laboratory of Electronics, MIT, Cambridge, MA*
[2] *12015 Ladrido Lane, Austin, TX 78727*
[3] *Ambridge University, Cloudcroft, NM 88317*

In previous work we reported observations of a thermal response from Pd cathodes electrolyzed in heavy water stimulated by a single diode laser. In more recent experiments, stimulation was done using two overlapping weak laser beams, and the cell was observed to respond to the difference frequency. The cell responded to three difference frequencies in the THz range at 8.2 THz, at 15.1 THz, and at 20.8 THz. The first two of these frequencies can be associated with optical phonon frequencies of PdD with zero velocity. We examine the conjectures that the response at 20.8 THz is due to deuterium in vacancies in the gold coating, or due to hydrogen contamination.

1. Introduction

It is probable that there has not been a more contentious issue in science over the last twenty years than the issue of the thermal response that has been claimed in experiments with Pd cathodes electrolyzed in heavy water. In this work, we describe results that we obtained in our experiments where we observed a version of the effect that seems to respond to the frequency difference between two weak lasers. The difference frequency in these experiments was in the terahertz regime, and the thermal response that we see appears to be correlated with characteristic frequencies associated with optical phonon modes.

Before proceeding, we need to give some account of what has gone on previously (at least from our perspective) in order to place the research under discussion in context. Experiments that seemed to show a large thermal effect for Pd cathodes in D_2O:LiOD were first described by Fleischmann and Pons in 1989 [1,2]. There were many attempts to replicate the experiment that followed shortly after the announcement [3,4], with the near-uniform result that no anomalous thermal effect was observed. In addition, strong arguments were made as to the impossibility of the claimed effects. Most physicists today consider the basic experiment to be irreproducible and the claimed effect impossible, which together constitutes reason to believe that the initial experiments showing a thermal effect were in error.

Some of those continuing to work on the Fleischmann-Pons experiment have argued that these early negative results need to be reconsidered in light of subsequent experimentation. According to this point of view, the basic Fleischmann-Pons ex-

periment was poorly understood in 1989 when many of these early experiments were done, and the success rate in Fleischmann and Pons' own experiments at that time was low.

In work carried out in the early 1990s at SRI, thermal effects were observed, and an attempt was made to correlate observations of excess power with the cathode loading (D/Pd ratio), current density, and other observables. It was found in these experiments that the cathodes which showed the effect had reached a very high loading (D/Pd = 0.95) early on, and that generally no effect was observed until about a month into the experiment in the case of cathodes that had maintained a high loading [5]. Further, a correlation was noticed between the amount of excess power produced during an event and the cathode loading during the event; significant excess power was higher for higher loading, with no effects seen at a loading below about 0.83 [6].

Some effort has been devoted to trying to understand the early negative results in light of the criteria derived from these early SRI experiments. As an example, in very few of the early negative results was any effort reported to monitor the loading; since at that time the loading was not generally considered to be an important variable to be controlled in the experiment. In the few cases where estimates were given (such as in [3]), the loading was well below that required to see the thermal effect. From this point of view, most of these early negative results are probably not relevant to the question of the thermal effect in the Fleischmann-Pons experiment, since essentially none of them were carried out in a relevant experimental regime. This reflects the general level of understanding of the experiment in 1989 when most of these early experiments were done (which was poor), rather than on the quality of the experiments or experimentalists (many of whom were very good).

In light of these comments, the most important negative result is that of Green and Quickenden [7]. High D/Pd ratios were reported in this work, consistent with the loadings in the SRI experiments where half or more of the cathodes were seen to give a thermal effect. Why the cathodes in these experiments gave no excess heat is not immediately clear. The protocol adopted in these experiments was different than in the SRI experiments, where current steps were used (rather than current ramps in the SRI experiments), and the maximum current density used was 300 mA/cm^2 (which is on the order of the threshold current density for some of the SRI experiments). In the SRI experiments, a correlation between excess power and deuterium flux has been observed; a current ramp gives a more sustained flux, which may be important. The duration of the SRI experiments tended to be longer (two months compared to one) than those of Green and Quickenden, which may be relevant given the late onset of excess power in the SRI experiments.

From the earliest days following the Fleischmann-Pons announcement, arguments have been made that the thermal effect itself is rather small; hence, there was good reason to believe that the thermal effect could be attributed to measurement error. Once again, this perception has persisted now for more than 20 years, and is presently widely accepted within the physics community. According

to Huizenga, it is the total energy which is important, rather than measurements of the excess power seen during a thermal event [4]. From this point of view, a thermal event in which excess power is observed at levels commensurate with the input power should not be considered relevant. Instead, the total energy associated with the thermal event (which might last 10 hours) needs to be weighed against the total energy put into the cell since the start of the experiment (which might be 6 weeks). So, in this way an effect which was considered by the experimentalists to be significant (a 100% power excess) thermal event, could be turned into an insignificant (1% energy excess) thermal event, which Huizenga could then argue was not within the measurement capability of the calorimeter involved.

We draw attention to the measurements described in [2] in which more than 4 MJ of energy was observed over 80 hours from a Pd cathode with a volume of 0.157 cm^3. Huizenga's stated concern was that it is possible that some unknown storage mechanism might be present, so that one could not be certain that net energy was produced. Although he did not specify what storage mechanisms he had in mind, if energy storage were to occur somehow in the cathode for this example, it would need to store about 60 MJ/cm^3; in our view this would constitute a remarkable effect in its own right worthy of study. The calorimetric approach which was pioneered by Fleischmann and Pons in association with these experiments was shown to give power balance to within about 0.1 mW in the case of a Pt cathode (which shows no thermal effect) [8].

There are by now numerous publications of observations of excess power in the Fleischmann-Pons experiment in the literature [9,10]. A large number of these are discussed in the review of [11]. Although we reject Huizenga's argument that only the energy gain should be considered in regard to the thermal effect, we draw attention to the observations of the Energetics group over the past several years; large thermal events have been reported in which the energy gain computed from the start of the experiment reached 2500% [12].

We see the thermal effect in our experiments. Our protocol is different from the Fleischmann-Pons protocol, so that an experiment can be done in a week rather than in 6 weeks. In earlier related experiments, the cell was seen to respond to the illumination of the cathode surface with a single weak diode laser [13,14]. Excess power at the level of a few hundred milliwatts was seen with laser illumination with mW lasers. This effect was confirmed at other laboratories [15,16,17,18]. In the new experiments two lasers are used under conditions where a single laser is unable to produce a response, so that both together trigger a thermal response when both are p-polarized, and when the beams overlap. The response is seen to depend on the difference frequency, which is in the THz regime in these experiments.

Why there should be a thermal effect in any of these experiments is not understood at present. However, it is clear that whatever physical process is responsible is unlike other condensed matter or nuclear processes that we are familiar with. To learn about the new effect, many experiments are going to have to be done to sort out how it works one issue at a time. The results reported here should be thought

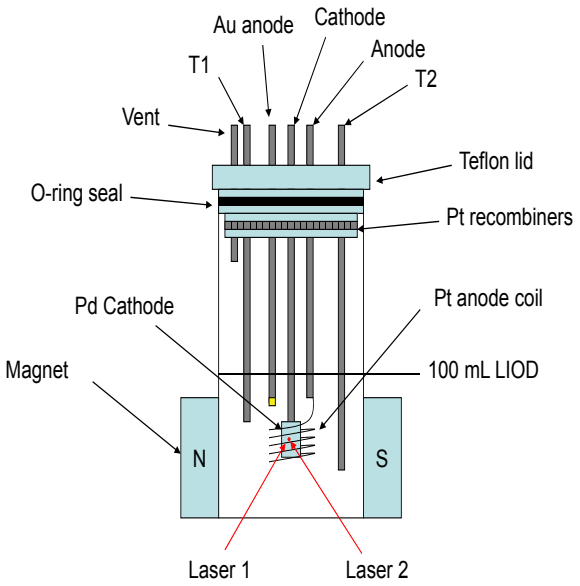

Figure 1. Schematic of the experimental set up.

of as one such step.

2. Overview of experiment

The experiment under discussion is an electrochemical cell with a Pd cathode and Pt anode in D_2O with 0.5 M LiOD (see Figure 1). The cathode is loaded at low current (0.050 Amps) for 120 hours, prior to the deposition of a gold coating and commencement of the thermal experiments at higher current (1.25-1.5 Amps).

2.1. *Outline of calorimetry*

Temperature measurements from inside and outside the cell are used in connection with Fick's law in steady state to estimate the thermal output power

$$P_{out} = K\Delta T \tag{1}$$

The input power is taken to be the electrical power minus the contribution of the thermoneutral potential

$$P_{in} = I(V - V_0) \tag{2}$$

The cell is closed in the sense that the D_2 and O_2 generated by the electrochemistry are recombined at the top of the cell; however, the heat generated during the recombination is poorly coupled back to the electrolyte. The excess power is estimated from

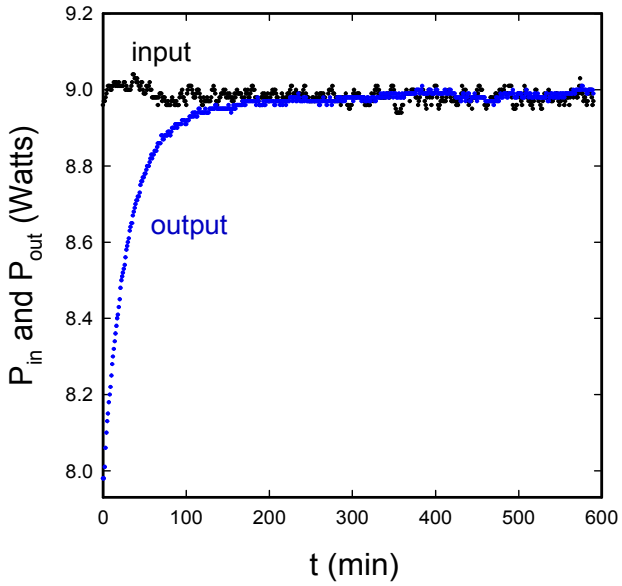

Figure 2. Measured input and output powers (watts) as a function of time (minutes). The error in the output power points is about 10 mW; the error for the input power points is much less.

$$P_{xs} \;=\; P_{out} - P_{in} \tag{3}$$

The calibration constant K is determined by running until steady state is reached prior to turning on the lasers (assuming no excess power); a check is made by running in steady state at the end of the experiment (again assuming no excess power). An example showing input and output power during a calibration run is shown in Figure 2.

An extended discussion of related experimental issues is given in the Appendices.

2.2. *Suppression of spontaneous excess power bursts*

Over the years in working with these cells, we have gotten a sense of how they respond to dual laser stimulation. In previous experiments at other laboratories, it was noticed that the excess power in the Fleischmann-Pons experiment responds to current density, such that the excess power is seen to increase roughly linearly above a threshold (which occurs in the general vicinity of 200-400 mA/cm for Pd rods [6]). As a result, the current density in this experiment provides for a way to control the response of the system, much like the knob on an amplifier controls how loud music is played. Our goal was to run the system just below threshold for spontaneous bursts of excess power (in order to suppress them), so that we might be able to see

more clearly the response of the system to laser stimulation. As the cathode area is about 1 cm^2 including front and back, the associated current density is about 1 A/cm^2; which is "low" for this experiment in the sense above.

A similar control is available in the operating temperature of the cell. Once a cell produces excess heat, often more excess heat can be seen if the cell temperature is increased. Of the operating temperatures available to us, we have purposely selected a lower operating temperature, again in order to help suppress unwanted spontaneous events.

3. Results

The primary result from this set of experiments is a spectrum of the excess power response as a function of difference frequency. To understand the significance of this spectrum, we need some explanation of how individual data points were obtained.

3.1. *Thermal response*

The construction of an accurate spectrum requires a degree of control which is probably beyond the current capability of any laboratory currently pursuing excess power in the Fleischmann-Pons experiment. We make no such claims here for our experiments. Nevertheless, our system has responded in a very reproducible way to the difference frequency between the two lasers, and this very much seems to be a real effect. As such, the effect can be quantified. We can measure the thermal response of the system in many experiments, and the difference frequency is available in these experiments. It seems clear that there is a thermal response in many of the experiments, and we have used simple relaxation models combined with a statistical analysis to quantify the excess power.

We consider in Figure 3 one of the better examples of how this works. Before the relative $t = 0$ of this figure, the cell was charged at low current density for a great many hours; a few hours before $t = 0$, the current was run up to about 1 A/cm^2, and the cell temperature was allowed to come to a steady state. Between minute 303 and 304, the two lasers were turned on, with a difference frequency of 20.66 THz. The excess power computed using the steady state calorimetry discussed above is seen to approach a constant power by about $t = 500$ minutes. The apparent excess power for this run as determined from a statistical fit to a simple relaxation model

$$P_{xs} \;=\; A + B(1 - e^{-(t-t_0)/\tau}) \tag{4}$$

(and shown in Figure 3) is 336 ± 8 mW. This value must be corrected to take into account the absorbed laser power (measured to be about 15 mW in other experiments), reducing it to 321 ± 8 mW. The relaxation time associated with this event is 43 minutes, which is longer than the calorimeter relaxation time (30 minutes) obtained from the data of Figure 2.

One can see a rapid transient in the data, which peaks at $t = 320$ minutes. This is the response of the system to a sudden drop in cell voltage (which we have verified),

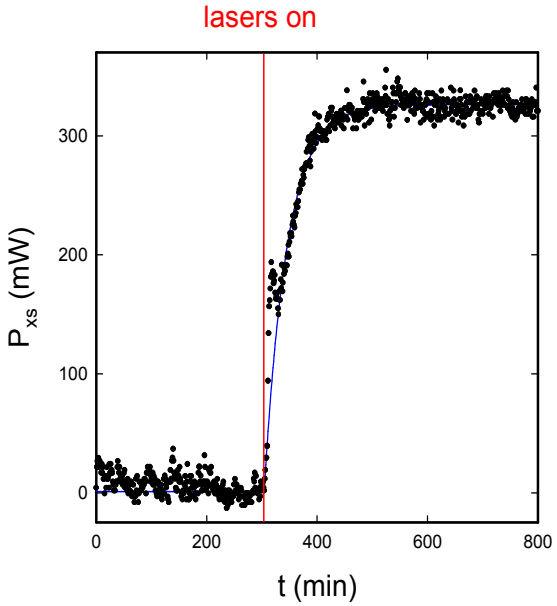

Figure 3. Excess power (mW) as a function of relative time (min) for parts of data set 662N2 and 662O2 (circles), along with a best fit relaxation model (curve). Two lasers were turned on between time 303 and 304, as indicated by the vertical line. The difference frequency is 20.66 THz.

which occurs in some of our experiments as a precursor to the onset of excess heat. The cell is run in a constant current mode from minute to minute, with the current set each minute to keep the power constant. When the cell voltage drops (and consequently the effective cell resistance drops), the electrical input power is a bit low, which leads to a transient difference between the output power (which changes slowly) and the input power (which is low transiently). In other experiments where excess heat is observed, such precursors are sometimes seen [19]. In Guruswamy and Wadsworth [20] there is an example of this where a sudden drop in the cell voltage preceeds an excess power burst. A precursor can be seen in the excess power data of McKubre et al [21]. Why the cell voltage drops is not known. It may be due to a change in the electrolyte conductivity, to a change in the overpotential of the cathode surface, or to significant change of the cathode surface temperature. It is probably easiest to measure the electrolyte conductivity directly to help clarify this, although we have not done this yet. Of interest is the possibility that the change is a surface effect connected with low-level energetic particle emission.

In this example, the system is seen to respond to the laser stimulation, starting from an initial condition of no excess power. The excess power following laser stimulation approaches nearly a constant value which we can determine by reference to a relaxation curve. There are 18 data sets of this type from the experiments. In addition, there are experiments in which the frequency was changed several times,

leading to excess power at different levels which appeared to correlate with the difference frequency. We have 37 excess power points obtained from these runs. For this data, we were able to compare the data against relaxation models in order to estimate the associated steady state excess power levels and standard deviations. In both cases the spread in excess power was similar, with values between 6 and 20 mW; in a few of the runs there are noticeable fluctuations in the excess power when high, and in some other runs the cathodes just seem to produce more noise. We note that there is a difference in the response generally observed from the different cathodes used to make up the spectrum. In some cases there is a slow drift in the calibration; consequently, we have added 10 mW systematically to the uncertainty for the data obtained from the scans since they are more sensitive to this drift.

Given these issues, as well as others that have not been discussed here, the spectrum that results should be regarded as preliminary. Where strong responses are observed, the confidence is highest; but more work is needed in order to clarify the response away from the peaks (the region most in need of such study is the region between 10 and 13 THz). However, as these experiments take a great deal of time and effort, a decision was made to present the data that we have so far as a preliminary result.

3.2. *Spectrum*

The spectrum that results from using this approach in a large number of experiments is shown in Figure 4. The spectrum appears to show three peaks near 8, 15 and 20 THz, which correspond to difference frequencies that we found in earlier experiments to give the best results. Due to constraints imposed by the lasers that we used, we were unable in these experiments to perform tests above 22.11 THz.

We have constructed a least squares fit to the the data points using a sum of three Lorentzians according to

$$P_{xs}(f) \;=\; \sum_j A_j \frac{\gamma_j^2}{(f-f_j)^2+\gamma_j^2} \tag{5}$$

where f is the difference frequency, where the A_j are amplitudes, where f_j are center frequencies, and where γ_j are width parameters. The fitting parameters that correspond to center frequencies and widths are given in Table 1. We have included the associated quality factor Q_j defined in terms of the fitting parameters according to

$$Q_j \;=\; \frac{f_j}{\gamma_j} \tag{6}$$

The line width of the 8.2 THz in the excess power spectrum is comparable to the 295 K line width near 9 THz measured in the coherent neutron scattering experiment of Rowe et al [22]. We have not found comparable results to compare with the other peaks, which have larger quality factors in the excess power spectrum.

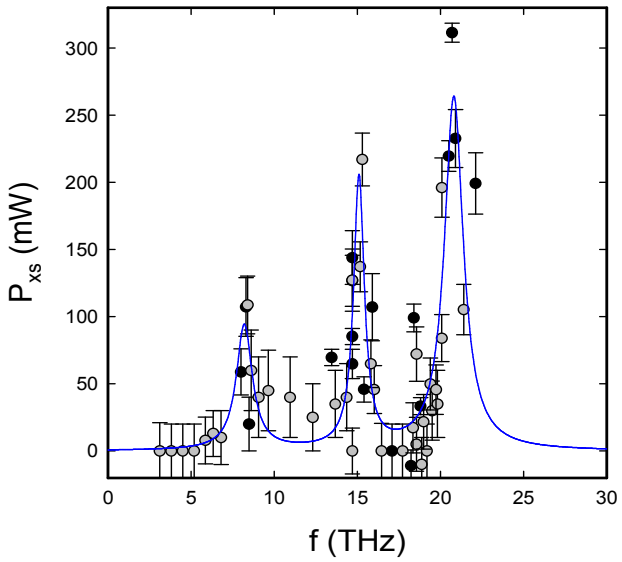

Figure 4. Excess power (mW) as a function of difference frequency (THz). Data from step results as in Figure 3 are in black; data from scans are in grey. Best fit of three Lorentzians shown as a solid line.

Table 1. Center frequency, width, and quality parameters for the excess power spectrum.

f_j(THz)	γ_j (THz)	Q_j
8.2	0.58	14
15.1	0.39	39
20.8	0.69	30

In this analysis, we have omitted one outlier data point at 14.75 THz where a response of 521 mW was observed; inclusion of this data point results in an increase of the amplitude of the middle Lorentzian by about 70 mW, but little change of the f_j or γ_j parameters. We have some data points from a scan between 10 and 13 THz where the excess power was close to zero, but these were not included because there was not a significant positive response at any of the scanned frequencies, which weakens the significance of the data.

We note that the fitting parameters obtained in this model-based statistical analysis are very close to the fitting parameters we obtained previously [23] based on a simple assignment of excess power numbers.

4. Discussion

These results are interesting for a number of reasons. There are the very practical issues that allow such an experiment to be done at all, and the perhaps unexpected result that the cathode seems to be able to respond to a difference frequency, even though the laser intensity is very low. Finally, there is the important question of the interpretation of these results.

4.1. *Practical issues*

Before a consideration of what the spectrum means, it seems useful to consider some practical issues associated with the experiments. In earlier single laser experiments, the excess power seemed to be similar once initiated, over about a factor of 50 in incident beam power. Hence, the concept of a threshold intensity for the effect seems to be relevant, with a threshold intensity in the general vicinity of 1 mW/cm^2. In different experiments, the same cathode was observed to respond when the beam was defocused to 1 cm diameter at a power level about 50% higher than when the beam was focused to 1 mm. This suggests that when the smaller beam is used, that an area larger than the beam responds, if we assume that the power produced per unit area is similar in the two cases.

All of this seems to be helpful in a practical sense over the course of the measurements. A relative insensitivity to the laser spot size and intensity of the lasers in these experiments is likely to have contributed to the quality of the resulting spectrum.

4.2. *Response to the difference frequency*

Under normal conditions, we would not expect the production of difference frequencies for optical laser light at the relatively low intensity of the light in this experiment. The intensity corresponding to the initial 30 mW beam power of a single laser focused to 1 mm diameter is about 4 W/cm^2.

One plausible route for the development of a nonlinearity is to assume that the codeposition of the gold results in irregular structures on the nano scale, so that a dramatic field enhancement occurs similar to the situation in surface enhanced Raman scattering [24,25,26]. In this picture, a large enhancement of the local electric fields results in strong excitation of local hybrid plasmon and optical phonon modes, allowing mixing at the difference frequency. In our experiments, we do not see a response at the difference frequency without gold codeposition.

We know from single laser experiments that excess power is produced. If we think of a laser amplifier as an analogy, then the amplifier tends to put energy into modes that have the highest excitation. In single laser experiments with the Fleischmann-Pons effect, such an analogy would suggest that the energy produced is going into the excited hybrid plasmon and optical phonon modes stimulated by the laser. These modes are very lossy, so that when the laser is turned off, the excess power effect is not sustained. In the two-laser experiments, the excess power

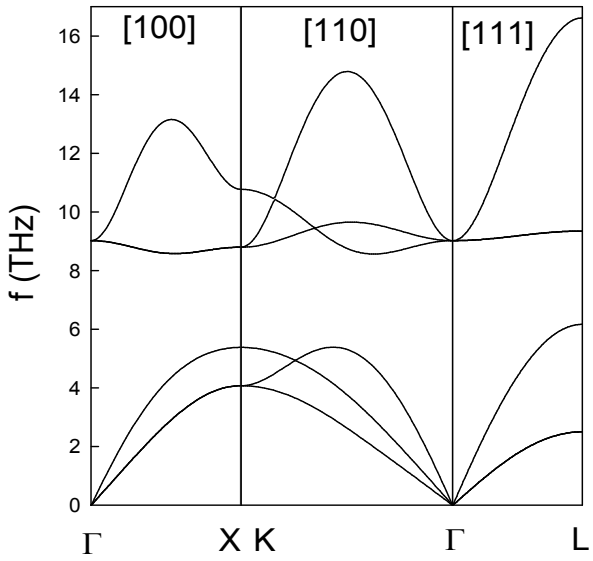

Figure 5. Phonon mode dispersion relation for PdD. Frequency in THz as a function of **k** for high symmetry directions in the Brillouin zone.

often remains after the lasers are turned off. The associated picture is that energy is going into these modes at a sufficient rate to sustain them, since they are at lower frequency and much less lossy.

4.3. *PdD optical phonon modes*

Since the thermal signal responds to difference frequencies in the THz region, it would be natural to make a connection with the relevant phonon mode spectrum in this region. In Figure 5 we have plotted the dispersion curves for the acoustical and optical phonon modes for the high symmetry directions in the Brillouin zone, using the Born-von Kármán fitting parameters of Rahman et al [27] with the modification for the D-D interactions of Sansores et al [28].

The lowest optical phonon frequency (8.57 THz) in the model occurs in the [110] direction, while the lowest points in the coherent neutron scattering experiments of Rowe et al [22] for $PdD_{0.63}$, and Blaschko et al [29] for $PdD_{0.78}$ are in the [100] direction, where the lowest model frequency is 8.58 THz. The loading in our experiments was not measured, but in other experiments where the loading was measured, excess heat usually does not appear until the loading is near 0.83 [6]. These lowest frequencies are for transverse modes; the lowest longitudinal optical phonon frequency occurs at the Γ-point, which in the model occurs at 9.02 THz. Both coherent neutron scattering experiments [22,29] agree in this case, but in [30] the Γ-point is observed in

$PdD_{0.63}$ at 8.1 THz at 80 K.

The group velocity is zero at this minimum, and also at the Γ-point. In the associated microscopic picture, the energy put locally into optical phonon modes with a finite group velocity would tend to transport away, while it would remain if the group velocity is zero. Given that there are numerous modes at different frequencies, it seems noteworthy that the thermal response in these experiments seems not only connected with the optical phonon modes, but those with zero group velocity.

A similar connection seems plausible between the thermal response at 15.1 THz and the longitudinal optical phonon mode at the L-point, which in the Born-von Kármán model occurs at 16.6 THz. Note that the model seems to be high relative to the L-point experimental data; which in the experiment of Rowe et al [22] seems to be closer to 16 THz; and in the experiment of Blaschko et al [29] seems to be closer to 15 THz. As has been emphasized by the ENEA Frascati group [18], the coupling of p-polarized light is with longitudinal plasmon modes, which we would expect to be hybridized with the optical phonon modes. The high frequency optical phonon mode at the L-point is a longitudinal mode, and once again the group velocity is zero at this point.

4.4. *Possibility of deuterium in vacancies in gold*

There are no optical phonon modes in PdD near 20.8 THz, which is the difference frequency associated with the third peak in the excess power spectrum shown above. One possible explanation is that the response is due to optical phonons associated with deuterium in gold. Since the solubility of deuterium in gold is low, this perhaps would not be a first choice for an explanation. However, since the gold codeposition may produce a large fraction of vacancies (as has been verified for Cu and Ni [31]), perhaps this is a possibility. The importance of vacancies in supporting regions of low electron density where molecular D_2 can bind has been discussed recently in [32]. Unfortunately, there does not seem to appear studies of hydrogen or deuterium in gold from which we can quantify the optical phonon spectrum.

Recent preliminary results by one of the authors (DL) with gold codeposition on copper suggests that the codeposited gold can produce a thermal response. If confirmed, then this would suggest that the issue of deuterium in gold should be pursued in the two-laser experiment.

4.5. *Possibility of hydrogen contamination*

A possible explanation for the response near 20.8 THz may be hydrogen contamination. We would expect some hydrogen contamination in the heavy water, the effect of which would be exacerbated by about an order of magnitude in palladium since the solubility of H in Pd is higher than the solubility of D (see the absorption isotherms of [33] in the beta phase region). The frequency of the longitudinal optical phonon mode at the L-point in PdH is about 20 THz, which seems encouraging.

In order to investigate further, we have run Born-von Kármán calculations for an idealized mixed crystal lattice with one deuterium atom in four replaced by a hydrogen atom (which would correspond to less than 3% contamination of light water in the electrolyte). If we make use of the force constants appropriate for PdD (since D is dominant), then we compute the frequency of the highest frequency longitudinal mode at the L-point to be 19.7 THz, which seems to compare favorably with the 20.8 THz response seen in the excess power spectrum.

It may be possible to clarify this issue in future experiments with reduced H contamination. If the thermal response is reduced or eliminated in cells that are relatively free of hydrogen, then this would support the conjecture that H is responsible for the 20.8 THz signal.

5. Conclusions

The thermal response in the Fleischmann-Pons effect has been sufficiently controversial over the years that much of the discussion has been focused on the question of whether the effect is real, or experimental error. Much less effort has been devoted to more general issues having to do with how it works; and the question of why it works has historically been relegated largely to speculation. In the experiments described here, we have found that the excess power depends on the difference between the optical frequencies of two lasers, which provides a new tool which can be used to gain information about the system that was previously unavailable. The spectrum that results suggests that optical phonon modes participate in our experiments.

Perhaps the most important feature of the excess heat in the Fleischmann-Pons experiment is that a very large amount of energy is produced (far in excess of what is possible from chemical reactions), yet no commensurate energetic particles are observed [34]. Energetic particles are observed at very low levels (more than 10 orders of magnitude below that required to be commensurate with the energy produced) under lower current density conditions where excess power would not be expected [35].

So, where does the energy go? For years it has been conjectured that the energy goes into low energy degrees of freedom associated with the solid, such as plasmon or optical phonon modes, prior to thermalization. In the experiments discussed in this work, there is indirect evidence that the energy produced is going into the optical phonon modes. The dependence on the difference frequency signals the presence of a nonlinearity, which is likely in the internal plasmon modes since the laser intensity is so low. The persistence of the the excess power after the lasers are turned off (an effect not typically associated with single laser experiments) suggests that the optical phonon modes are being sustained by the energy source.

Appendix A. Electrochemical issues

The experimental results discussed in this paper came from 20 tests conducted on 3 electrochemical cells using lithium deuteroxide as electrolyte and palladium

cathodes. The experiments began in March 2007 and paused in May 2007, resuming in April 2008 and continue to the present. All experiments were conducted in Austin, Texas using the experimental setup shown below in Figure 1.

Appendix A.1. *Cells:*

The cells used were 200 mL capacity Kimax electrochemical cells, stock number 14020 and made of borosilicate glass. The cells were approximately 11 cm tall and 6 cm in diameter. The cells were fitted with a Teflon plug which made an airtight seal, using a standard #127 Buna O-ring as shown schematically in figure 1. A 2 mm groove was cut below the O-ring seal to hold the recombiner catalyst (see Figure 1).

The cells were equipped with 5 mm glass tubing that served as electrode holders and O-ring sealable pass-throughs for hook up wires and thermistors. A vent tube was open to the atmosphere and provided pressure relief in the event of recombiner failure. The cells were also equipped with a second anode, which could be connected to the positive side of the electrolysis power supply using a solid state relay. The second anode, when activated, provided for in-situ plating of gold onto the cathode during electrolysis.

The cell lid is machined Teflon, sealed using rubber o-rings. The electrode holders are 5mm diameter soft glass tubing obtained from Richland Glass. The end of the glass tubing in the electrolyte is sealed against a platinum hook-up wire to provide mechanical stability and to keep the cell sealed. The tubing end outside of the cell is sealed with a commercial epoxy.

Appendix A.2. *Cathode:*

The cathodes were all bulk palladium and were typically 5 mm x 12mm x 0.20 mm of 0.999 purity. Our sources for the anode and cathode material vary but Alfa-Aesar and Metallium are two commonly-used vendors. The cathode fabrication process is as follows: cut 10 mm x 5 mm x 0.5 mm billet from 10 mm x 10 mm x 10 mm source; polish to bright using a Dremel brush with aluminum oxide; rinse in tap water; heat in furnace to 750 C for 3 hours, then cool slowly (4-8 hours); etch with aqua regia for 2 minutes at 100 C; polish with Dremel metal brush with aluminum oxide; polish with Dremel fiber brush with aluminum oxide; ultrasonic clean for 5 minutes in tap water; anneal for 2.5 hours at 850 C; polish with Dremel metal brush (Nicksand); ultrasonic clean for 5 minutes using compound remover; cold roll to about 0.25 mm, turning sample 90^o on each of 4 passes; polish with Dremel metal brush; ultrasonic clean for 5 minutes using compound remover; anneal for 2.5 hours at 850 C; etch with aqua regia for 2 minutes at 100 C; rinse in distilled water.

Appendix A.3. *Anode:*

The anodes were all coils of 0.999 pure Pt wire obtained from Alfa Aesar, with a wire anode diameter of 0.5 mm, and with four turns over the cathode.

Appendix A.4. *Electrolyte:*

All experiments were conducted using 100 mL of D_2O with 0.5 M LiOD. Heavy water was obtained from Sigma Aldrich, 99.9 atom% D, stock number 151882-500g, batch 05512EE. Lithium granules were also obtained from Sigma Aldrich, 99.9+%, stock number 499811-25g, batch 02313TC.

Appendix A.5. *Recombiner:*

All cells were run in a closed cell configuration. The gasses produced were recombined using small platinum coated pellets. The pellets were obtained from Alfa Aesar, 0.5% Pt on 1/8 inch Alumina, stock number 89106, lot B17Q15.

Appendix A.6. *Loading:*

Cell No. 662 is typical for this series of experiments. It was loaded for 120 hours at 0.05 amps. The loading ratio was not measured during the experiment but our experience has shown that loading in this manner usually results in a cathode that will respond to single or dual laser stimulation. After the cathode is loaded at low current, we increase current to 1 amp for 24-48 hours before plating gold on the cathode.

Appendix A.7. *Gold coating:*

In previous work it was observed that adding a thin layer of gold electrochemically to the surface was required in order to see a thermal response in single laser experiments [13]. To the upper left of the cathode (see Figure 1), is an electrode holder with a small piece of 0.999 purity gold attached to a platinum hookup wire. In our experiments, the gold plating occurs following the initial 120 hour charging period. This was done by adding the Au anode in parallel to the Pt anode, and running for a shorter time at a high current density (usually at 1 amp). As yet we have not determined how much gold ends up on the surface, but in our experiments we deposit gold until the cathode surface has turned dark.

What the gold coating does is not understood at present. Electrochemical deposition on a rough surface would not be expected to result in a uniform layer, and initial observations at NRL support this. Gold clusters on mica show a broad plasmon absorption feature near 2.5 eV in electron energy loss spectra [24,36], and it is possible that this helps in the absorption of the laser light. If there is separation on the nanoscale, one might expect field enhancements characteristic of surface enhanced Raman scattering [24]. The gold may also inhibit cathode deloading.

Appendix A.8. *Power:*

Power to the electrolytic cell and the controlled temperature enclosure is provided by twin HP digital power supplies, model number E3632A. The power supplies

can provide low ripple DC in constant current or constant voltage mode from 0-7 amps, 0 to 30V over two power ranges. Labview controls the power supplies and the electrolysis cell is run in constant power mode, with the power supply set in constant current mode. Cell power is controlled to within ±0.01W.

Appendix B. Calorimetric issues

Simple Fick's law calorimetry as described in the text was used on all tests, consistent with the set-up illustrated in Figure 1.

Appendix B.1. *Temperature measurements:*

Two Beta Therm thermistors were used to measure cell temperature in two locations within the cell - one slightly above the cathode and one slightly below the cathode. The manufacturer provided thermistor calibration constants. The cells were not mechanically stirred; however, the mixing efficiency is reflected by the low temperature gradient between the two probes - typically 0.1 C or less. The temperature difference ΔT is taken to be the average of the internal cell temperatures minus the enclosure ambient temperature, which is a two-thermistor average also. We found that ΔT was typically 30-35 C.

Appendix B.2. *Thermal control:*

Lab temperature was fairly stable at 26 ± 1 C. The cell was kept in a controlled environment where airflow was constant and ambient temperature was maintained at 25 ± 0.03 C.

Appendix B.3. *Cell power:*

Cell power was provided by a digital HP E3632A DC power supply, at typically 7-10 watts, with current up to 1.25 or 1.5 amps. The cell power was held constant by Labview to about 10 mW.

Appendix B.4. *Calorimetric scheme:*

The excess power during the live part of the experiment is estimated through

$$P_{xs} \;=\; P_{out} - P_{in}$$

as discussed in the text. Note that the cell has a recombiner, and under normal operating conditions all of the deuterium and oxygen are recombined. When the recombiner begins to fail, then gas is lost through a vent. This gas goes through a bubbler, so that we are able to see easily when this happens. The recombiner provides a heat source with power IV_0, which in our experiments has proven to be nearly constant. Running near 1 A means that 1.54 watts is generated in the recombiner, most of which is lost. About 60 mW of this power makes it back to the cell, resulting in a constant temperature increase of about 0.25 C.

Appendix B.5. *Calibration:*

A cell is run for many hours prior to turning on the lasers. We estimated the calibration constant K assuming that no excess power was present during this initial stage. The calibration constant was computed again at the end of the experiment (typically well after any thermal signals had died out), generally with good agreement between the two values. The onset of each thermal event was readily observed since transients stand out against the nearly constant zero excess power background. Variations in the excess power output during the zero excess power phase of the experiment is around 10 mW and was dominated by variations in the input power; consequently we have taken 10 mW for the error associated with the excess power measurements in steady state.

This simple method of determining excess power does not take into account the thermal relaxation time of the system; the response of the calorimeter to a constant power input is shown in Figure 2. Constant power input is applied by measuring the current and voltage once per minute, determining the effective cell resistance, and then fixing the current to the square root of power divided by this resistance. This results in the spread in input power seen in the figure.

Appendix B.6. *Data collection:*

An Agilent 34970A and takes measurements every minute; the cell and box temperature measurements are made with the Agilent. The Agilent also provides voltage to control solid state relays used to start and stop in-situ gold plating.

Appendix C. Lasers

Dual tunable lasers were used to provide beat frequencies in the 3 to 24 THz range. The laser diodes are off-the-shelf red diodes from various manufacturers such as Sony, Hitachi and Panasonic. One laser is controlled using an Optima LDC202 with a laser mount that accepts 5.6mm laser diodes. The LDC202 is controlled by providing DC voltage from the Agilent to set laser current and temperature. Our laser diodes typically operate at 70 mA and tune over a temperature range of 15-40C. The second laser control system is an ILX3722B laser controller and laser mount. It operates by GPIB and can handle 5.6mm or 9 mm laser diodes. It can tune over 0 to 60C, producing a typical tuning range of 4-6 nm. Both instruments were controlled by Labview to drive the lasers at the desired wavelengths. The output power of the diode lasers was about 2030 mW each when new before 2002, and both combined produced close to 25 mW at the end of the experimental campaign. The linewidth was 1 nm.

Appendix C.1. *Difference frequency:*

For difference frequencies in the range of 15-20 THz, we used one laser typically centered near 685 nm, and another laser centered near 658 nm; both lasers could

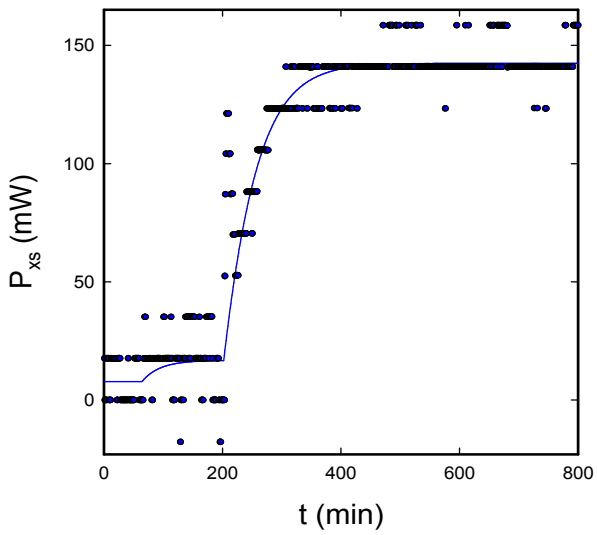

Figure 6. Excess power (mW) as a function of time (min) for parts of data set 662J-K. The lasers were turned on at minute 64 with mismatched polarization, indicated by the first step. The polarization of one of the lasers was rotated at minute 202, indicated by the onset of a major increase in the relaxation model fit. This gave rise to a prompt (artifact) apparent increase with excess power, which can be attributed to a sustained reduction in cell resistance; and then a subsequent increase in excess power. The spread in the excess power around the model is 9 mW. Data was saved with too few digits when this experiment was run, resulting in the discretization of the points that can be seen in the figure.

be tuned over 4-6 nm. For observations near 8 THz, we used a third laser centered at 664 nm.

Appendix C.2. *Laser diagnostics:*

The output power of the laser diodes was measured using an Ophir power meter. The wavelengths were determined using a Stellarnet optical spectrometer, which has a resolution of about 0.25 nm.

Appendix C.3. *Beam overlap:*

The second beam was aligned to overlap with the first on a single spot on the cathode surface roughly 1 mm in diameter.

Appendix C.4. *Polarization:*

As noted above, we needed to have both laser beams incident with p-polarization relative to the surface. This was accomplished using a half-wave filter. The lasers

were oriented at wide angles to the cell so that the incident angle was greater than 45^o relative to the cathode surface. The effect of laser polarization can be seen in Figure 6. At 64 minutes (when two overlapping laser beams with mismatched polarization and a difference frequency of 14.88 THz) one can see a minor increase of the P_{xs} signal, which is on the order of the absorption of the laser power in the cell. At 202 minutes the polarization of one of the lasers was rotated by 90^o, at which point both laser beams were overlapped on the surface with p-polarization. The system responds slowly, reaching an excess power of about 140 mW by about 400 minutes (which is significantly longer than the response time of the calorimeter). This data supports the notion that the polarization of both lasers is important in producing an excess power response. Between 64 minutes and 202 minutes both lasers were on and tuned to produce a difference frequency near the middle resonance, yet there was no strong response. The system only responded strongly when both lasers have p-polarization, which occurred at 202 minutes.

A prompt apparent excess power spike can be seen in the data following the rotation of the laser polarization. This is due to a sudden drop in the cell voltage which appears sometimes as a precursor to an excess power event as discussed in the text.

Appendix D. Magnets

We used two permanent magnets (approximately 700 Gauss) on either side of the cell during the thermal measurements, but these are not in place during the (preceding) loading phase. The magnets seemed to help in obtaining a thermal response, and the effect was independent of the orientation. There is some evidence that the alignment of the laser polarization with the magnetic field is important. In the present experiments the magnetic field lines are horizontal and extend along the cathode surface; the laser beams come in horizontally, at an angle of about 45^o from the cathode surface; in p-polarization, the magnetic field of the light is vertical.

The magnets in this experiment are a legacy from earlier single laser experiments where, in some experiments, they seemed to help. Magnets appear to make a difference in the Pd morphology in the codeposition experiments described in [35]. In future work we hope to understand better how the magnetic field impacts the two-laser experiment.

References

1. M. Fleischmann, S. Pons, M. Hawkins, J. Electroanal. Chem. **261**, 301 (1989); errata **263**, 187 (1990).
2. M. Fleischmann, S. Pons, M. W. Anderson, L. J. Li, M. Hawkins, J. Electroanal. Chem. **287**, 293 (1990).
3. N. S. Lewis, C. A. Barnes, M. J. Heben, A. Kumar, S. R. Lunt, G. E. McManis, G. M. Miskelly, R. M. Penner, M. J. Sailor, P. G. Santangelo, G. A. Shreve, B. J. Tufts, M. J. Youngquist, R. W. Kavanagh, S. E. Kellogg, R. B. Vogelaar, T. R. Wang, R. Kondrat, R. New, Nature **340**, 525 (1989).

4. J. R. Huizenga, *Cold Fusion, the scientific fiasco of the century*, (University of Rochester Press, Rochester, 1992)
5. M. C. H. McKubre, F. L. Tanzella, Using Resistivity to Measure H/Pd and D/Pd Loading: Method and Significance, *Twelfth International Conference on Cold Fusion, Condensed Matter Nuclear Science, Yokohama*, edited by A. Takahashi, K.-I. Ota, and Y. Iwamura (World Scientific, 2005), p. 392.
6. M. C. H. McKubre, S. Crouch-Baker, A. M. Riley, S. I. Smedley, F. L. Tanzella, Excess Power Observations in Electrochemical Studies of the D/Pd System; The Influence of Loading, *Third International Conference on Cold Fusion, Frontiers of Cold Fusion, Nagoya* edited by H. Ikegami, (Universal Academy Press, Tokyo, 1993) p. 5.
7. T. A. Green, T. I. Quickenden, J. Electroanalytical Chemistry **389**, 91 (1995)
8. M. H. Miles, M. Fleischmann, Accuracy of Isoperibolic Calorimetry Used in a Cold Fusion Control Experiment, *Low-energy nuclear reactions sourcebook, ACS Symposium series* **998**, (Oxford University Press, Oxford, 2008) p. 153.
9. M. C. H. McKubre, S. Crouch-Baker, R. C. Rocha-Filho, S. I. Smedley, F. L. Tanzella, T. O. Passell, J. Santucci, J Electroanal. Chem. **368**, 55 (1994).
10. D. Gozzi, F. Celluchi, P. L. Cignini, G. Gigli, M. Tomellini, E. Cisbani, S. Frullani, G. M. Urciuoli, J Electroanal. Chem. **452**, 251 (1998).
11. E. Storms, *Science of Low Energy Nuclear Reaction: A comprehensive compilation of evidence and explanations about cold fusion*, (World Scientific Publishing Co, Singapore, 2007).
12. I. Dardik, T. Zilov, H. Branover, A. El-Boher, E. Greenspan, B. Khachaturov, V. Krakov, S. Lesin, M. Tsirlin, Excess Heat in Electrolysis Experiments at Energetics Technologies, *Eleventh International Conference on Cold Fusion, Condensed Matter Nuclear Science, Marseilles*, edited by J. P. Biberian, (World Scientific, 2004), p. 84.
13. D. Letts, D. Cravens, Laser Stimulation of Deuterated Palladium: Past and Present, *Tenth International Conference on Cold Fusion, Condensed Matter Nuclear Science, Cambridge, MA*, edited by P. L. Hagelstein and S. R. Chubb, (World Scientific, 2003), p. 159.
14. D. Cravens, D. Letts, Practical Techniques in CF Research: Triggering Methods, *Tenth International Conference on Cold Fusion, Condensed Matter Nuclear Science, Cambridge, MA*, edited by P. L. Hagelstein and S. R. Chubb, (World Scientific, 2003), p. 171.
15. E. Storms, Use of a Very Sensitive Seebeck Calorimeter to Study the Pons-Fleischmann and Letts Effects, *Tenth International Conference on Cold Fusion, Condensed Matter Nuclear Science, Cambridge, MA*, edited by P. L. Hagelstein and S. R. Chubb, (World Scientific, 2003), p. 183.
16. M. McKubre, F. Tanzella, P. L. Hagelstein, K. Mullican, M. Trevithick The Need for Triggering in Cold Fusion Reactions, *Tenth International Conference on Cold Fusion, Condensed Matter Nuclear Science, Cambridge, MA*, edited by P. L. Hagelstein and S. R. Chubb, (World Scientific, 2003), p. 199.
17. M. R. Swartz, Photo-Induced Excess Heat from Laser-Irradiated Electrically Polarized Palladium Cathodes in D_2O, *Tenth International Conference on Cold Fusion, Condensed Matter Nuclear Science, Cambridge, MA*, edited by P. L. Hagelstein and S. R. Chubb, (World Scientific, 2003), p. 213.
18. M. Apicella, E. Castagna, L. Capobianco, L. DAulerio, G. Mazzitelli, F. Sarto, A. Rosada, E. Santoro, V. Violante, M. McKubre, F. Tanzella, C. Sibilia, Some Recent Results and ENEA, *Twelfth International Conference on Cold Fusion, Condensed Matter Nuclear Science, Yokohama*, edited by A. Takahashi, K.-I. Ota, and Y. Iwamura (World Scientific, 2005), p. 117.
19. D. Cravens, D. Letts, The Enabling Criteria of Electrochemical Heat: Beyond Rea-

sonable Doubt, *Fourteenth International Conference on Cold Fusion* (in press).
20. S. Guruswamy, M. E. Wadsworth, Metallurgical Aspects in Cold Fusion Experiments, *First Annual Conference on Cold Fusion, Salt Lake City*, edited by F. Will, (National Cold Fusion Institute, 1990), p. 314; see Figure 2(c).
21. M. C. H. McKubre, R. C. Rocha-Filho,S. Smedley, F. Tanzella, J. Chao, B. Chexal, T. Passell, J. Santucci, Calorimetry and Electrochemistry in the D/Pd System, *First Annual Conference on Cold Fusion, Salt Lake City*, edited by F. Will, (National Cold Fusion Institute, 1990), p. 20; see Figure 5.
22. J. M. Rowe, J. J. Rush, H. G. Smith, M. Mostoller, H. E. Flotow, Phys. Rev. Lett. **33**, 1297 (1974).
23. D. Letts, D. Cravens, and P.L. Hagelstein, "Dual Laser Stimulation and Optical Phonons in Palladium Deuteride, in Low-Energy Nuclear Reactions and New Energy Technologies," *Low-Energy Nuclear Reactions Sourcebook* Volume 2, American Chemical Society: Washington DC. p. 81-93 (2009).
24. K.-H. Su, Q.-H. Wei, X. Zhang, J. J. Mock, D. R. Smith, S. Schulz, Nano Letters **3**, 1087 (2003).
25. D. A. Genov, A. K. Sarychev, V. M. Shalaev, A. Wei, Nano Letters **4**, 153 (2002).
26. X.-M. Qian, S. M. Nie, Chemical Society Reviews **37**, 912 (2008).
27. A. Rahman, K. Sköld, C. Pelizzari, S. K. Sinha, H. Flotow, Phys. Rev. B **14**, 3630 (1976).
28. L. E. Sansores, J. Tagüeña-Martinez, R. A. Tahir-Kheli, J. Phys. C: Solid State Phys. **15**, 6907 (1982).
29. O. Blaschko, R. Klemencic, P. Weinzierl, L. Pintschovius, Phys. Rev. B **24**, 1552 (1981).
30. J. M. Rowe, J. J. Rush, J. E. Schirber, J. M. Mintz, Phys. Rev. Lett. **57**, 2955 (1986).
31. Y. Fukai, M. Mizutani, S. Yokota, M. Kanazawa, Y. Miura, T. Watanabe, J. Alloys and Compounds **356-357**, 270 (2003).
32. P. L. Hagelstein, I. U. Chaudhary, "Arguments for Dideuterium near Monovacancies in PdD," *Proc. 15th International Conference on Cold Fusion* (in press)
33. R. Lässer, K.-H. Klatt, Phys. Rev. B **28**, 748 (1983).
34. P. L. Hagelstein, to appear in *Naturwissenschaften*.
35. P. A. Mosier-Boss, S. Szpak, F. E. Gordon, L. P. G. Forsley, European Physics Journal: Appl. Phys. **40** 293 (2007).
36. S. Holst, W. Legler, Z. Phys. D **25**, 261 (1993)